Available online at www.sciencedirect.com
SCIENCE DIRECT
Cement and Concrete Research 35 (2005) 167–176
CEMENT AND CONCRETE RESEARCH

Percolation of capillary pores in hardening cement pastes

Guang Ye*

Magnel Laboratory for Concrete Research, Department of Structural Engineering, Ghent University, Technologiepark-Zwijnaarde 904 B-9052, Ghent (Zwijnaarde), Belgium

Received 28 April 2004; accepted 19 July 2004

Abstract

This paper presents a study of the pore structure and permeability of hardening cement pastes. Cement pastes with water/cement (w/c) ratio 0.4, 0.5 and 0.6 from 1 up to 28 days of age were tested with mercury intrusion porosimetry. In parallel, the water permeability was measured. With the help of a numerical simulation model, correlations between pore structure and permeability were found. Water permeability is related more to the pore size distribution and to the effective porosity than to the total porosity of the pastes. No depercolation of the capillary pores was evident neither in the experiments nor in the numerical simulations during the first 28 days after casting.

Keywords: Cement paste; Porosity; Permeability; Percolation; Modelling

1. Introduction

The percolation theory [1] deals with disordered multiphase media in which the disorder is characterized by the degree of connectivity of the phases. In percolation studies, one is often interested in the fraction of a phase that is connected across the microstructure as a function of the total volume of the phase [2]. The microstructure of cement-based materials provides numerous examples of percolation phenomena, such as percolation of the CSH and CH phases and percolation of the capillary pores phase [2–4]. In particular, the depercolation of the capillary pores is of great interest for studying the transport phenomena in cement-based materials.

The application of the percolation theory for explaining the transport properties and, in particular, the permeability of cement-based materials can be summarized as follows. In the initial stage of cement hydration, the capillary pores are all connected, and the cement matrix has a high permeability. With the increase of the degree of hydration, capillary pores decrease in volume and size and start to become disconnected; as a consequence, the permeability decreases as well. At a certain degree of hydration, the capillary pores are not connected any more, so that no connected path exists for the capillary transport; the result is a significant and sudden reduction in permeability. The value of the porosity at this hydration stage is called the "depercolation threshold".

Important investigations about the influence of percolation on capillary transport in cementitious materials date back to the early 1950s, when Powers et al. [5,6] described the degree of hydration to achieve segmentation of the capillary pores in Portland cement pastes as a function of water/cement (w/c) ratio (Table 1).

From the results of water permeability measurements, Powers et al. [6] concluded that the capillary pores in cement paste exhibit a percolation transition from connected to disconnected at about 20% porosity. This means that, regardless of the w/c ratio, when the capillary porosity in cement paste drops to 20%, no capillary transport is possible. The water permeability dramatically falls down to a certain value around 10^{-14} m/s when the capillary pores become depercolated. On the other side, whenever the measured permeability reached that value, depercolation of capillary pores had occurred.

* Tel.: +32 9 264 5523; fax: +32 9 264 5845.
E-mail address: ye.guang@UGent.be.

0008-8846/$ - see front matter © 2004 Elsevier Ltd. All rights reserved.
doi:10.1016/j.cemconres.2004.07.033

Table 1
Curing time and degree of hydration capable of segmenting the capillary pores in a Portland cement paste, according to [6]

w/c Ratio	Degree of hydration (%)	Curing time
0.40	50	3 days
0.45	60	7 days
0.50	70	14 days
0.60	92	6 months
0.70	100	1 year
>0.70	100	Impossible

However, the water permeability of cement paste reported by other authors shows significant variations (Fig. 1). For example, parallel measurements of porosity and permeability by Mehta and Manmohan [9] showed discrepancies with Powers' conclusion. Their experimental results indicated that the depercolation threshold of capillary porosity did not occur in cement pastes with w/c ratio above 0.30, even at ages up to 1 year [9]. Results by Banthia and Mindess [7] show similarities with Mehta and Manmohan's [9] for samples with w/c 0.35 at a curing age of 30 days. Detailed investigations have shown that the variations in water permeability are largely dependent on a series of factors, i.e., type of media (O_2, N_2, water or other liquid solutions) used in permeability tests [10], sample preparation [11], influence of curing conditions (sealed or saturated) and age of the sample and the pressure used in the permeability tests [7].

The existence of a percolation threshold of the capillary pores in cement paste appears to be both a relevant and a controversial subject. This study aims at exploring this phenomenon with experiments and with numerical simulations. Systematic experiments on pore structure and water permeability of cement pastes were conducted for cement paste samples with water/cement ratio 0.4, 0.5 and 0.6 at curing ages of 1, 3, 7, 14 and 28 days. Three-dimensional (3D) microstructures of the cement pastes were simulated,

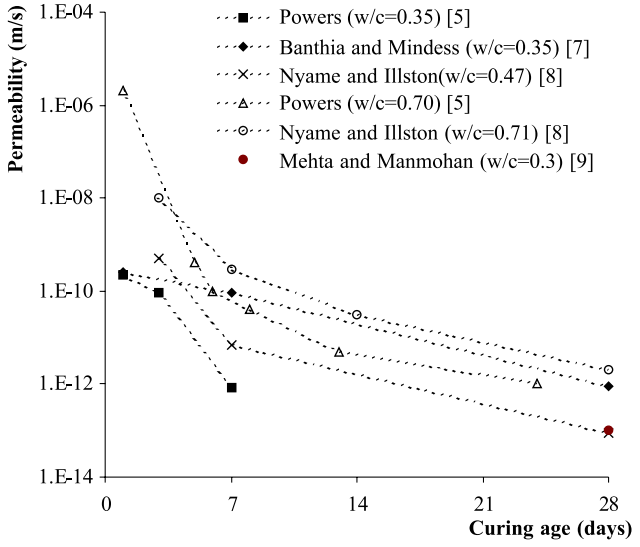

Fig. 1. Comparison of permeability values reported by different authors.

Table 2
Chemical composition of CEMI 32.5R cement

Analyte (oxide)	Mass (%)
CaO	63.4
SiO_2	21.0
Al_2O_3	5.03
SO_3	3.0
Fe_2O_3	2.83
MgO	2.0
Na_2O	0.24
K_2O	0.65
TiO_2	0.30
P_2O_5	0.16
Mn_2O_3	0.06
f_{CaO}	0.5
Total	99.17

and the depercolation of the capillary pores was analyzed. Experimental results and numerical simulations are discussed in this paper and compared with other results in the literature.

2. Experiments

The experimental section includes two major parts. The first part concerns pore-structure measurements using mercury intrusion porosimetry (MIP). The second part deals with the percolation phenomenon as determined from permeability tests.

The cement paste specimens were prepared with Portland cement, CEM I 32.5R by ENCI. The chemical composition of the cement is listed in Table 2. The calculated four main constituents according to modified Bogue equations [12] are listed in Table 3. These values are used as input for the numerical simulations.

Cement pastes with three different w/c ratios, i.e., 0.4, 0.5 and 0.6, were used for both MIP measurements and permeability tests. The degree of hydration of cement paste was calculated using the HYMOSTRUC model [13] and was calibrated by heat release measurements of cement pastes using an isothermal calorimeter up to 14 days of age (Fig. 2).

2.1. Mercury intrusion porosimetry measurements

2.1.1. Sample preparation

The cement paste used for MIP measurements was mixed with deaerated distilled water in a standard 5-l epycyclic

Table 3
Constituents of CEM I 32.5R cement

Phases	Mass (%)
C_3S	63
C_2S	13
C_3A	8
C_4AF	9

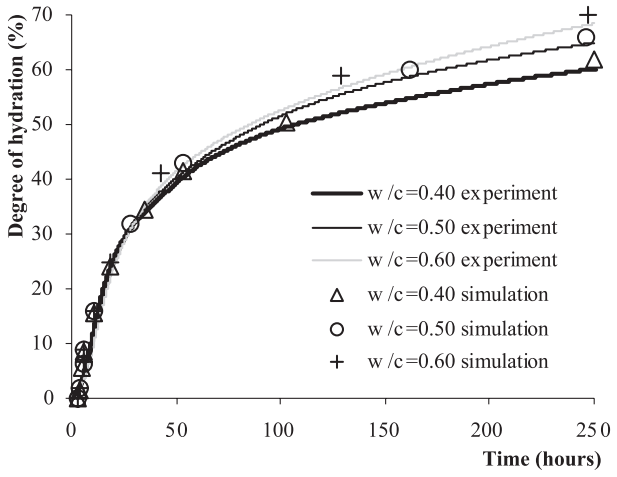

Fig. 2. Degree of hydration of cement paste as a function of time.

mixer. After 1 min of mixing at low speed and 2 min of mixing at high speed, the pastes were poured into 500-ml glass bottles. The bottles were vibrated to remove air bubbles and then sealed with a tight plastic cover. The samples were then rotated at a speed of 5 rpm in a room at 20±1 °C for 24 h. This procedure minimizes possible bleeding and segregation in the cement paste. After rotation, the bottles were moved into a climate box at 20±0.1 °C until the age of testing.

Curing periods of 1, 3, 7, 14 and 28 days were considered. At the end of each curing period, the glass bottle was broken, and the sample was removed from the bottle and split into small pieces of about 1 cm^3. The split samples were exposed to freeze–drying with liquid nitrogen. The whole drying procedure was the same as suggested by Gallé [14].

Mercury intrusion measurements were performed with a Micromeritics PoreSizer 9320. The PoreSizer 9320 is a 207-MPa mercury intrusion porosimeter that is able to resolve pore sizes in the range of 7 nm to 500 μm. A measurement is conducted in two stages: a manual low-pressure run from 0 to 0.17 MPa and an automated high-pressure run from 0.17 to 205 MPa. Data are collected and handled by a computer acting as a control module.

Thanks to the extended capacity of the porosimeter, the whole MIP test procedure, including the first intrusion, the extrusion and the following second intrusion, was performed on the same sample. The curves of mercury intrusion and the extrusion hysteresis can be obtained this way. In the hysteresis curve, the continuous and the inkbottle pores are detected in the first intrusion. In fact, all pore space is assumed to be filled with mercury at the end of the first intrusion. When the pressure is released, mercury is sucked out of all pores, except of the inkbottle and dead-end pores. The volume of the removed mercury is defined as 'effective porosity', which corresponds to the part of the porosity relevant for the transport properties [17]. If the mercury is repressurized, the pore size distribution of effective porosity can be obtained from the second intrusion curve [16].

2.2. Permeability measurements

The permeability apparatus is shown schematically in Fig. 3. The system includes a regulated gas pressure source, a gas/water reservoir, three parallel permeability cells, a computer controlling system and appropriate valves and tubing.

2.2.1. Permeability cells

The specimens tested are cement paste disks with a diameter 95 mm. The thickness varies from a maximum of 50 mm to a minimum of 10 mm according to the sample used. They are inserted into a ring of Room Temperature Vulcanised silicone rubber with an outer diameter 150 mm and inner diameter 95 mm. The ring is confined by a steel-confining cylinder with inner diameter 200 mm and length 80 mm.

Two fitted end plates are provided to prevent axial length changes of the rubber ring, thus, it is forced to expand radially and seal the annular space between the specimen and the steel cylinder. The specimen itself is not subjected to mechanical load. The top plate is connected with the pressure source supply, while the bottom plate is connected with a needle outlet. Below the needle outlet, plastic

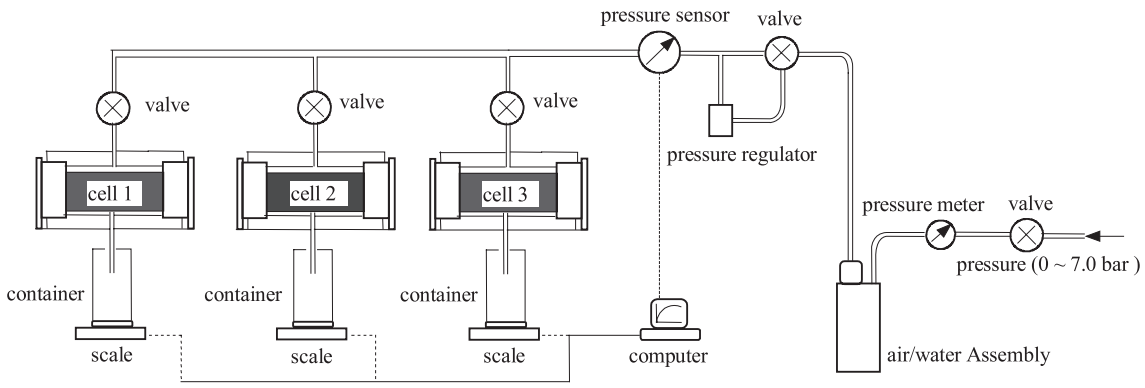

Fig. 3. Schematic view of the system for testing permeability of cement paste.

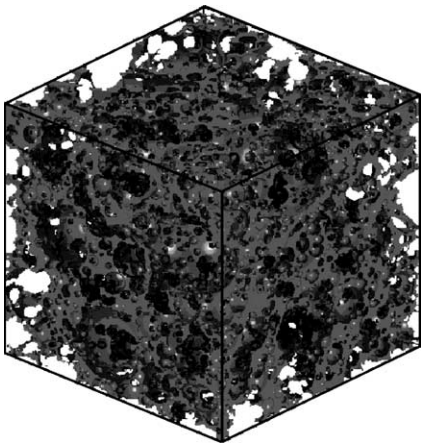

Fig. 4. 3D simulated pore structure (w/c=0.4, Φ_c=15%).

containers collect the water passing through the samples. A porous steel disk was placed as a support between the specimen and bottom plate to prevent cracking of the samples.

2.2.2. Data acquisition system

The data acquisition system consists of the electronic balances (±0.1 g) for weighing the water collected in the containers and is connected to an industrial computer. The system is programmed to allow independent start and stop for each cell. The scanning sequence and timing are set at the start of a test by defining either an interval of time or a weight change. Graphs showing cumulative collected water versus time for each cell are plotted on the computer screen. Achievement of a steady flow state can be observed directly from the plots.

2.2.3. Sample preparation and curing

Sample preparation and curing were almost the same as for the MIP test. In this way, it was possible to correlate the pore structure data with the permeability of the cement paste. However, small differences were needed because of the specific requirement of the permeability test, as mentioned in the following.

Samples for the permeability test were cast into PVC cylinders with length 800 mm and inner diameter 95 mm.

After casting and vibration, the cylinders were sealed to prevent moisture loss and were rotated for 24 h at 5 rpm to avoid segregation. After the 24-h rotation, the specimens were cured in a climate box at 20±0.1 °C. At each curing age, four disks with a thickness of 15 mm were sawn from the cylinders. The samples were then immersed in water and vacuumed for 4–8 h to saturate the samples. One of the samples was used for verifying the water saturation. The other three samples were moved into the permeability cells for the water permeability tests.3D microstructural simulation of cement paste.

3. 3D microstructural Simulation of Cement Paste

The 3D microstructure of cement paste was simulated and analyzed with the HYMOSTRUC3D model [13,18]. In the HYMOSTRUC3D model, the hydration of cement paste is simulated as a function of the particle size distribution and the chemical composition of the cement, the w/c ratio and the reaction temperature. The model starts from the cement particle size distribution in a 3D body, where the cement particles are represented by spheres. Upon contact with

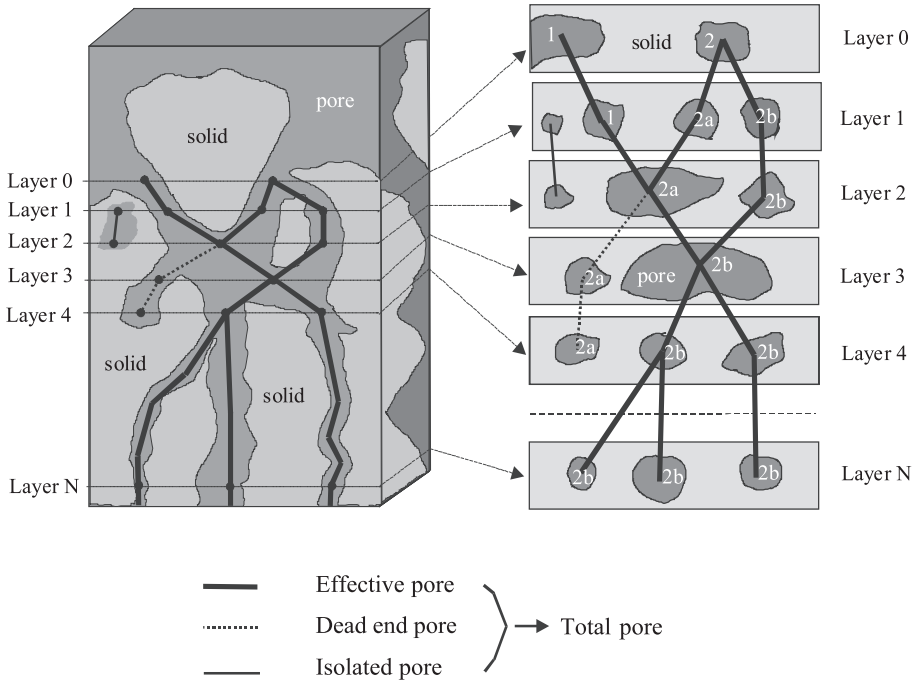

Fig. 5. Pore network structure determined by overlapping criterion; distinction between effective pores, dead-end pores and isolated pores.

water, and based on an interaction–expansion mechanism, the cement grains gradually grow. With progress of the reaction process, the growing particles become more and more connected. In this way, a simulated porous microstructure is formed. Fig. 4 shows an example of a simulated pore structure of a cement paste with w/c ratio 0.4 at a porosity, Φ_c, of 15%.

To assess the connectivity and percolation of capillary porosity, a serial section algorithm associated with an overlap criterion is employed. The connectivity of the capillary pore network is thus obtained, and a link list pore network structure is built (see Fig. 5). The depercolation of capillary porosity is analyzed based on the connectivity of the capillary pore network. In the simulation, the effective porosity is obtained as the volume of the pores through which water flow can occur (see Fig. 5, block line). Detailed information on the geometrical and topological parameters of the simulated microstructure, such as porosity, effective porosity, pore size distribution and connectivity of pores, is obtained with the algorithm described in Ref. [17]. The results, especially the connectivity of the capillary porosity, are largely dependent both on the image resolution of the slices (layers) and on the layer depth. The layer depth is the distance between neighboring slices, e.g., layers 0 and 1 in Fig. 5, left. The influence of image resolution and layer depth on the microstructural properties will be discussed further.

4. Results and discussion

The simulation and experimental results on the pore structure and the measured permeability results are summarized in Table 4. A good agreement in the total porosity was found between experiments and simulations.

4.1. Measured porosity and permeability

The relationship between permeability and total porosity, measured by MIP, is illustrated in Fig. 6, which shows the results for the samples with different water/cement ratios. It is clear that the permeability changes of the cement paste are primarily caused by the change of the pore structure. It is thus expected that a sample with higher porosity would be more permeable. However, Fig. 6 indicates that the relationship between porosity and permeability is not unique. For example, for the same MIP porosity of 39%, the permeability of the sample with w/c ratio 0.4 is one order of magnitude higher than for the sample with w/c 0.6. Thus, the porosity is not the only factor that determines the permeability. This is in agreement with the findings of Mehta and Manmohan [9].

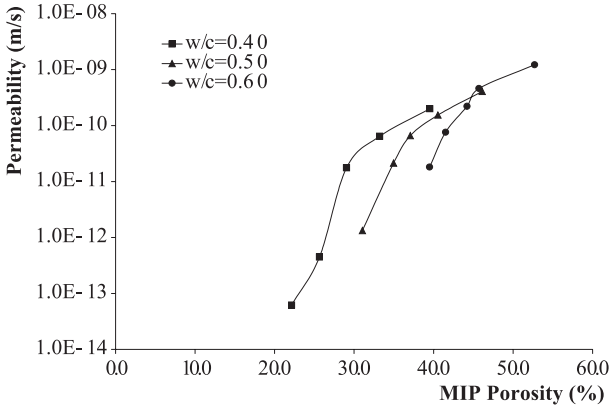

Fig. 6. Relationship between permeability and total porosity measured by MIP.

Table 5 lists the pore structure properties measured by MIP and the measured permeability of cement pastes with w/c ratio 0.4 at 1 day, w/c ratio 0.5 at 3 days and w/c ratio 0.6 at 28 days. They all have nearly the same capillary porosity, around 40%. However, when the sample with w/c ratio 0.4 is compared with the sample with w/c ratio 0.6 (Fig. 7), the sample with w/c ratio 0.6 at 28 days shows, on average, smaller pores. The critical pore diameters (defined as the pore width corresponding to the highest rate of mercury intrusion per change in pressure [15]) decrease even more, from 540 to 35 nm. Although the total porosity is the same, the pore size distribution can differ significantly. The fact that the w/c ratio 0.6 sample had much lower permeability implies that finer pore systems in cement pastes lead to lower permeability, even if the porosity is the same.

Table 4
Degree of hydration, porosity and permeability of cement pastes as a function of time

w/c Ratio	Age (days)	Degree of hydration (%)		Total porosity (%)		Effective porosity (%)		Permeability (m/s)
		Measured	Simulated	Measured	Simulated	Measured	Simulated	Measured
0.4	3	45.1	45.6	33.2	32.1	22.2	29.1	6.42×10^{-12}
	14	64.1	64.8	29.1	26.0	19.3	23.5	4.48×10^{-13}
	28	–	72.1	22.1	21.0	11.3	16.8	9.00×10^{-14}
0.5	3	46.2	46.4	40.5	41.4	27.3	40.8	1.54×10^{-10}
	14	68.9	69.2	35.0	32.1	20.9	30.9	2.14×10^{-11}
	28	–	77.2	31.1	28.9	17.0	25.8	1.33×10^{-12}
0.6	3	47.3	48.2	45.7	46.0	33.7	45.5	4.61×10^{-10}
	14	73.6	73.8	41.5	40.2	26.0	39.1	7.61×10^{-11}
	28	–	84	39.5	36.5	23.0	34.2	1.82×10^{-11}

Table 5
Pore structure and permeability of three different cement pastes with approximately the same porosity

Sample	Porosity (%)	Average pore diameter (nm)	Critical pore diameter (nm)	Permeability (m/s)
w/c 0.4 at 1 day	39.52	56	540	2.00×10^{-10}
w/c 0.5 at 3 days	40.54	56.4	380	1.54×10^{-10}
w/c 0.6 at 28 days	39.50	40.6	35	1.82×10^{-11}

When the pore structure parameters and permeability of cement pastes with w/c 0.4 at 1 day and w/c 0.5 at 3 days are compared (see Table 5 and Fig. 8), both samples show a similar pore size distribution and similar value of the average and the critical pore diameters. Most importantly, the measured permeability of the two samples was nearly the same. Thus, regardless of water/cement ratio and curing age, the water permeability of cement pastes appears to depend critically on the pore size distribution and connectivity of the capillary pores.

4.2. Percolation of capillary porosity from simulations

In this section, the simulation results on the percolation of capillary porosity with HYMOSTRUC3D will be discussed and compared with similar results from the CEMHYD3D [19,20] and Navi and Pignat's [21,22] models.

For samples with w/c ratio 0.3 and 0.4, Fig. 9 shows the capillary pore phases simulated with CEMHYD3D and with HYMOSTRUC3D. Note that in the CEMHYD3D model, only four sizes of particles were used, with diameters of 3, 9, 13 and 19 pixels. The size of the sample was $100\times100\times100$ μm^3, and the resolution in this case was 1 μm/pixel [20]. In HYMOSTRUC3D, a continuous particle size distribution, between 1 and 45 μm, was used. The size of the sample was the same as in the CEMHYD3D simulation. The image resolution was 0.25 μm, but the layer depth was 1 μm.

Significant differences in the simulated evolution of the capillary pore structure between the two models are shown in Fig. 9b. For cement paste with w/c ratio 0.4, the capillary pore space percolation threshold is found at about 20–22% porosity in CEMHYD3D [19], whereas in HYMOSTRUC3D, the percolation threshold of the capillary porosity is found at about 5% porosity. In fact, the pore space percolation threshold occurs in the CEMHYD3D simulation at a degree of hydration of 0.7, whereas in HYMOSTRUC3D, the capillary porosity percolation threshold occurs much later, at a degree of hydration around 0.9 (Fig. 9a). The cement paste with w/c ratio 0.3 simulated by HYMOSTRUC3D shows a depercolation threshold at a degree of hydration 0.68, where the capillary porosity was also around 5%. The virtual pore structure at this point is shown in Fig. 10.

The reason for the pronounced differences in the structure of the capillary pores in the two models lies in the different principles on which the two hydration models are based. In fact, both the morphology of the hydration products and the location where they are precipitated are different in the two models. In the CEMHYD3D model, the cement components are simulated as different sets of digital pixels. For example, when C_3S hydrates, a cellular automaton algorithm is applied in which the reactants (pixels) dissolve from their matrix and walk around in the capillary water space. When two reactants meet at a certain place, a chemical reaction occurs, and the reaction products, CSH and CH, are formed. The CSH gel forms mostly near anhydrous particles, and CH is located in the free pore space. Consequently, in CEMHYD3D, CSH is not concentrically and uniformly distributed around the particles; moreover, CH and other crystalline products are formed

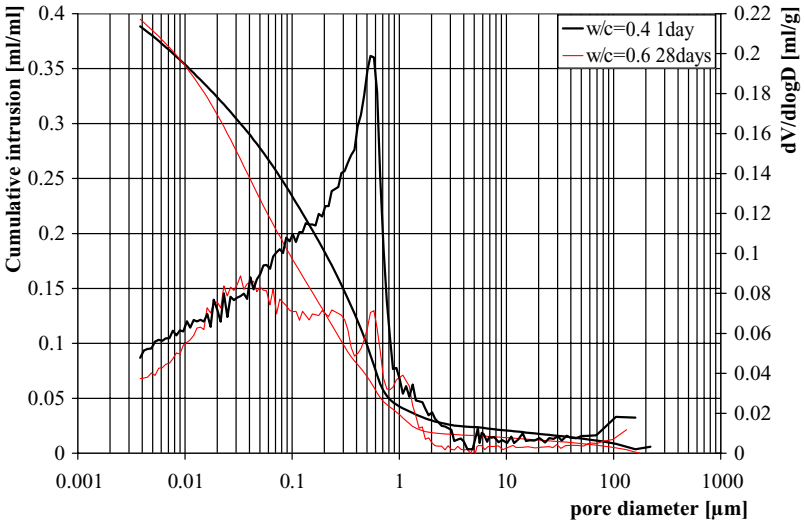

Fig. 7. Comparison of pore structure of cement pastes with w/c ratio 0.4 at 1 day and w/c ratio 0.6 at 28 days.

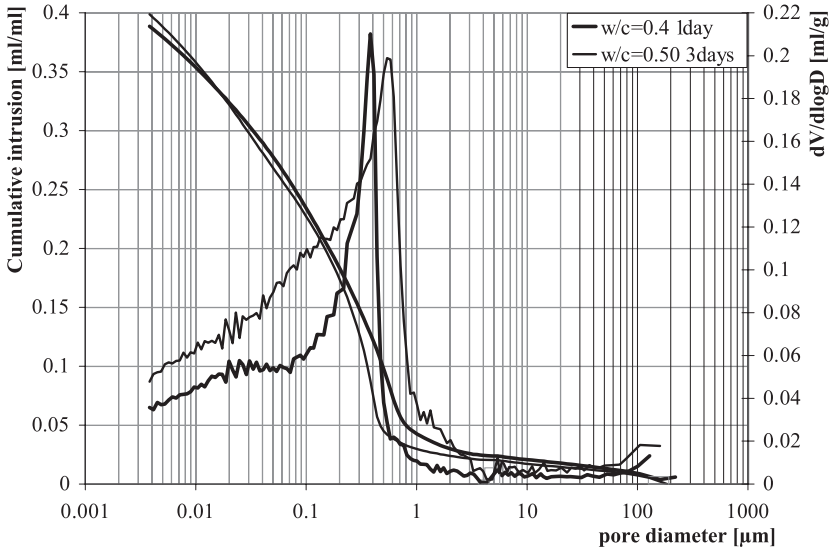

Fig. 8. Comparison of pore structure of cement pastes with w/c ratio 0.4 at 1 day and w/c ratio 0.5 at 3 days.

directly in the pores. In other models, such as HYMOSTRUC or Navi and Pignat's model [21], cement particles are simulated as spheres and hydration products as concentrical spherical shells. The growing spherical shells are overlapping when cement hydration takes place.

Another important factor that affects the capillary pore space percolation is the digital resolution. Fig. 11 presents the connected porosity fraction as a function of the degree of hydration calculated by HYMOSTRUC3D. Both the image resolution and layer depth were, in this case, 0.25 μm/pixel. It is noticed that, for all samples, the capillary pores are almost always connected, even at the ultimate degree of hydration. These results, implying that no depercolation of capillary porosity can be found, are quite different from the result of the CEMHYD3D model [20], but similar to previous results by Navi and Pignat [22]. For example, Navi's model showed that the percolation threshold of the capillary pore space changed from 30% to 12% to 0% porosity when the digital resolution increased from 10 to 5 to 2 μm/pixel for a cement paste with water/cement ratio 0.4. Also in the CEMHYD3D pixel-based simulation model [20], the percolation threshold of the capillary porosity changed from 24% to 18% to 11% if the digital resolution shifted from 1 to 0.5 to 0.25 μm/pixel in a cement paste with w/c ratio 0.30. This can be explained because smaller pores can be resolved at the greater resolutions, and the pathways that would seem to be closed at low resolution are seen to be open at higher resolutions. In the present simulation, the digital resolution was 0.25 μm/pixel; at this high digital resolution, even very small capillary pathways were detected, leading to a very low percolation threshold of the capillary porosity or no threshold at all [20].

It can be concluded that the connectivity of the pores is strongly influenced by the image resolution both in digital image- and spherical-based models. To accurately define the digital resolution, one should also consider the computational time and the reliability needed in the calculation result. On the other hand, a more realistic shape of the cement particles, like adoption of nonspherical particles [24], is a promising improvement to produce a realistic microstructure of cement paste, with direct influences on the capillary percolation.

In any case, if one uses the simulated pore structure for predicting the transport properties, the accuracy of the simulated pore structure will directly influence the reliability of the calculated water permeability. For validating the predicted percolation threshold of the capillary porosity, permeability experiments become necessary.

4.3. Percolation of capillary porosity and permeability

In the discussion above, some open issues remain about the use of the percolation theory to explain capillary transport in cement-based materials. In particular, both the occurrence of depercolation of the capillary pores for a given cement paste and the value of the porosity when it occurs seem to be unresolved issues. Moreover, the actual value of the permeability when the capillary pores are depercolated appears to be another debated subject.

The first question has a logical answer: Because the cement paste can be considered as a random porous material, in theory [23], a depercolation threshold always exists if the porosity is continuously decreasing. However, the real issue is how to determine the actual depercolation threshold value in practice from permeability tests. These issues are of great interest in view of validating a permeability model. In fact, most researchers [25,26] have followed the conclusion of Powers et al. [6]: "the capillary porosity in cement paste exhibits a percolation transition (from connected to disconnected) at a volume fraction of about 20% porosity". Powers and Brownyard [27] deduced this value from water permeability tests: Because the

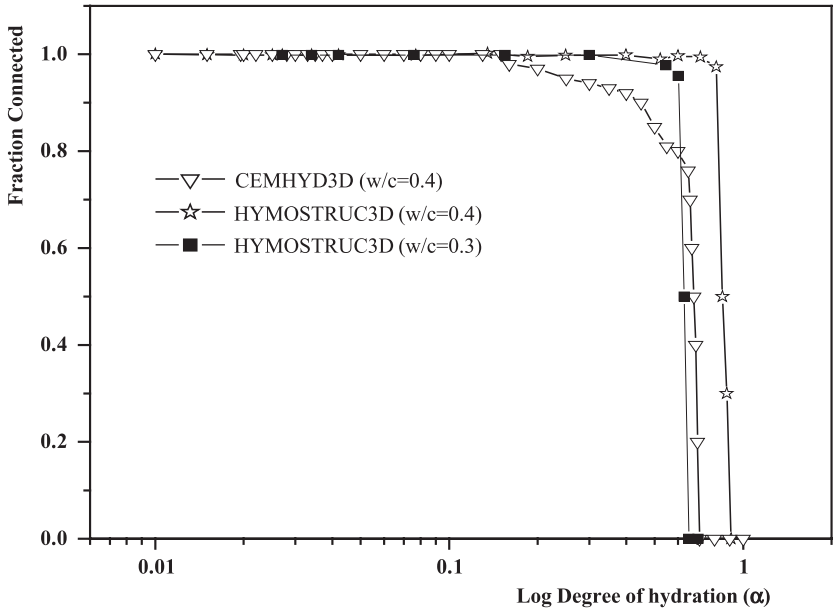

a) Connected volume fraction of pore phases at different degrees of hydration

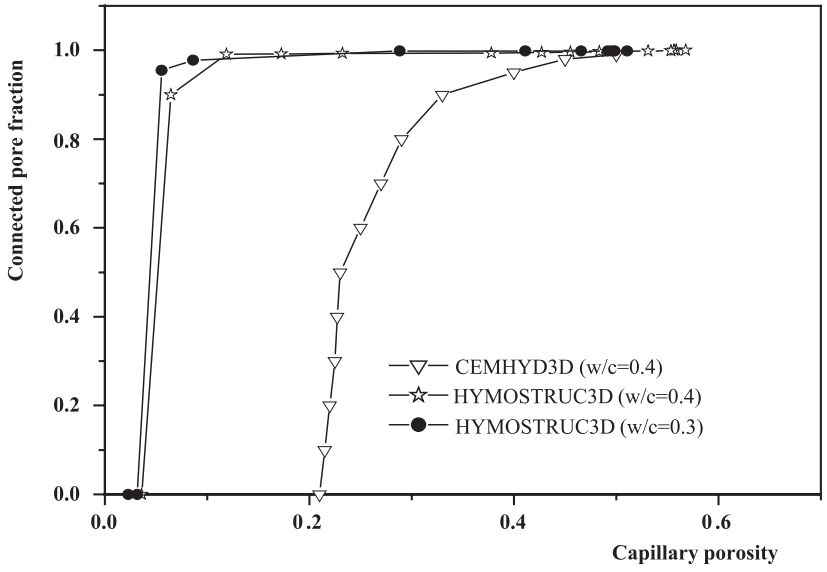

b) Percolation threshold of the capillary pores

Fig. 9. Development of the microstructure of cement pastes simulated by HYMOSTRUC3D and CEMHYD3D (resolution 1 μm/pixel). (a) Connected volume fraction of pore faces at different degrees of hydration. (b) Percolation threshold of the capillary pores.

capillary pores are approximately one or two order of magnitude larger than the gel pores are, when the capillary pores are connected, the water transport is dominated by them and the permeability is higher. When the capillary pores become disconnected, the gel pores will play a key role for water penetration. The minimum capillary permeability of cement paste, according to Powers et al. [6], is around 2.54×10^{-14} to 2.54×10^{-15} m/s. Once the permeability drops to this value in an experiment, it is possible to infer that the capillary pores in the cement matrix are depercolated. The value of the porosity at this moment is therefore the depercolation threshold.

Now, according to the results of the permeability experiments presented in Table 4, the lowest measured permeability is 9×10^{-14} m/s for the sample with w/c ratio 0.4 at 28 days. This value is higher than reported by Powers [6]; thus, no depercolation of capillary porosity was found. The result that no depercolation of capillary porosity was found for the sample with w/c ratio 0.4 at 28 days is also confirmed by results reported by Metha and Manmohan [9] (see Table 6). Applying the definition of depercolation threshold by Powers to their results, the capillary porosity should be less than 6.7%. This value is much lower than the value reported by Powers himself, 20% porosity. Thus,

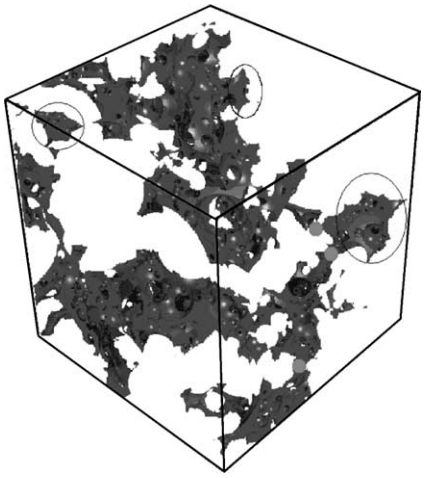

Fig. 10. Simulated capillary pore structure of sample with w/c ratio 0.30 at degree of hydration α=0.68.

Table 6 shows that the depercolation threshold of capillary porosity did not occur in cement pastes with w/c ratio above 0.3, even at ages up to 1 year. Measured permeability by other authors also supports this conclusion (see Fig. 1).

The difference between Powers' results [6] and the results reported in this study, as well as the results reported by Mehta and Manmohan [9], due to the fact that the experimental procedures, specially the curing condition, were different. As discussed above, the measured permeability of cement paste are much influenced by curing condition. In Powers' experiments [5], the cement pastes were cured with a water flow (can be treated as saturated condition) through it to leach out all alkali. This method, however, does not quite correspond to the field conditions. In the present study, the cement paste samples were cured under a sealed condition. Both with experiments and simulations, Bentz [28] has demonstrated that when samples are cured in saturated conditions, the degree of hydration of

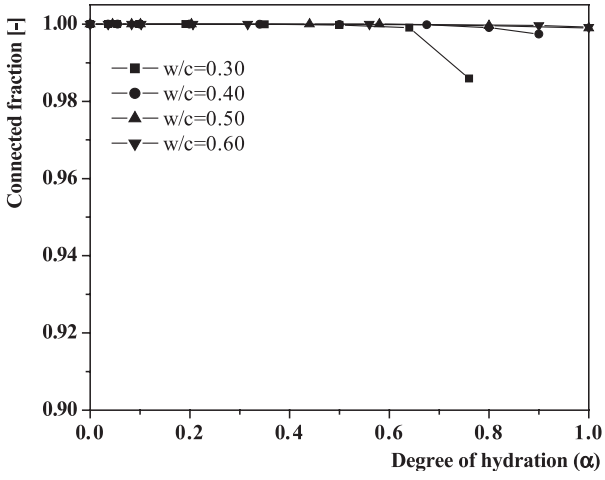

Fig. 11. Connectivity of capillary pores in cement pastes as function of the degree of hydration simulated by HYMOSTRUC3D (resolution 0.25 μm/pixel).

Table 6
Characterization of cement paste and permeability, after Ref. [9]

w/c Ratio	Age	Bulk density (g/cm^3)	Total porosity (cm^3/cm^3)	Degree of hydration (%)	Permeability 10^{-13} (m/s)
0.3	28 days	1.89	NA	54.6	1.0
	90 days	1.88	7.82	57.3	0.6
	1 year	1.94	6.70	64.7	0.4
0.4	28 days	1.65	NA	61.9	2.0
	90 days	1.70	11.53	64.7	1.0
	1 year	1.75	10.51	71. 6	1.0
0.5	28 days	1.50	19.73	64.2	3.0
	90 days	1.57	16.11	71.1	3.0
	1 year	1.57	15.73	75.2	1

the sample is much higher compared with sealed curing. The pore structure also shows a significant difference in his simulation. In a sealed system, empty pores are created as the hydration proceeds. As hydration continues, the empty pores occupy an ever-increasing fraction of the remaining total porosity. This may explain why the permeability measured in this study is much higher than that of Powers.

On the other hand, the numerical simulation provides an alternative tool in discovering the percolation phenomena in cement paste. The simulation results of the pore structure by HYMOSTRUC3D provided similar results. The capillary depercolation was found in the simulation for the sample with w/c ratio 0.3 at a degree of hydration of 68%, where the porosity was about 5% (see also Fig. 9). This value is close both to the observations in Ref. [9] and to the permeability measurements reported in this paper.

5. Conclusions

From this study, it was found that pore size distribution, critical pore diameter and effective porosity are the crucial factors that determine the water permeability. No depercolation of the capillary pores was found in the experiments for all samples with w/c ratio 0.4 to 0.6 up to a curing age of 28 days. The results are in good agreement with Refs. [6–9], but distinct from Powers' result. According to the simulated pore structure generated by HYMOSTRUC3D, the depercolation of capillary porosity occurs at about 5% porosity, corresponding to a degree of hydration 0.68 for samples with w/c ratio 0.3. This result is in agreement with experiments by Mehta and Manmohan [9], according to whom the depercolation threshold of the capillary pores for a sample with w/c ratio 0.30 after 1 year was less than 6.7%. Percolation of capillary pores simulated by different numerical models shows different result. This is due to significant influences of the image resolution and also to the principles on which the model is based. Numerical simulation results about depercolation of capillary pores presented in this paper are fundamental for developing and tuning permeability models for cement pastes and concrete.

Acknowledgements

The authors are very grateful to Dr. P. Lura for his useful suggestions and critical reading of the manuscript. This research was financially supported by the Dutch Technology Foundation (STW), which is gratefully acknowledged.

References

[1] D. Stauffer, A. Aharony, Introduction to Percolation Theory, 2nd ed., Taylor and Francis, London, 1992.
[2] D.P. Bentz, Fibers, percolation, and spalling of high performance concrete, ACI Mater. J. 97 (3) (2000) 351–359.
[3] D.P. Bentz, E.J. Garboczi, Percolation of phases in a three-dimensional cement paste microstructural model, Cem. Concr. Res. 21 (1991) 324–344.
[4] G. Ye, P. Lura, K. van Breugel, A.L.A. Fraaij, Study on the development of the microstructure in cement-based materials by means of numerical simulation and ultrasonic pulse velocity measurement, Cem. Concr. Compos. (2004) (in press).
[5] T.C. Powers, L.E. Copeland, J.C. Hayes, H.M. Mann, Permeability of Portland cement paste, J. ACI 51 (1955) 285–298.
[6] T.C. Powers, L.E. Copeland, H.M. Mann, Capillary continuity or discontinuity in cement pastes, PCA Bull. 1 (110) (1959) 2–12.
[7] N. Banthia, S. Mindess, Permeability measurements on cement paste, Proc. Material Research Society Symposium, Pore Structure and Permeability of Cementitious Materials, vol. 137, 1988, pp. 173–178, Pittsburgh.
[8] B.K. Nyame, J.M. Illston, Capillary pore structure and permeability of hardened cement paste, Proc. 7th International Congress on the Chemistry of Cement, Septima, Paris 3 (4) (1980) 181–185.
[9] P.K. Mehta, C. Manmohan, Pore size distribution and permeability of hardened cement paste, 7th International Congress on the Chemistry of Cement, Paris, France 3 (7) (1980) 1–5.
[10] R.D. Hooton, What is needed in a permeability test for evaluation of concrete quality, Proc. Material Research Society Symposium, Pore Structure and Permeability of Cementitious Materials, vol. 137, Materials Research Society, Pittsburgh, 1988, pp. 141–150.
[11] D. Hillel, Soil and Water, Physical Principles and Processes, Academic Press, New York, 1971.
[12] H.W.F. Taylor, Modification of the Bogue calculation, Adv. Cem. Res. 2 (6) (1989) 73–78.
[13] K. van Breugel, Simulation of hydration and formation of structure in hardening cement-based materials, Dissertation, Delft University of Technology, The Netherlands, 1991.
[14] C. Gallé, Effect of drying on cement-based materials pore structure as identified by mercury intrusion porosimetry: a comparative study between oven-, vacuum-, and freeze-drying, Cem. Concr. Res. 31 (10) (2001) 1467–1477.
[15] D.N. Winslow, S. Diamond, A mercury study of the evolution of porosity in cement, ASTM J. Materials (3) (1970) 564–585.
[16] D. Winslow, Some experimental possibilities with mercury intrusion porosimetry, Proc. Material Research Society Symposium, Pore Structure and Permeability of Cementitious Materials, vol. 137, 1988, pp. 93–104, Pittsburgh.
[17] G. Ye, K. van Breugel, A.L.A. Fraaij, Three-dimensional microstructure analysis of numerically simulated cementitious materials, Cem. Concr. Res. 33 (2) (2003) 215–222.
[18] G. Ye, Experimental study and numerical simulation of the development of the microstructure and permeability of cementitious materials. PhD thesis, Delft University of Technology, Delft, 2004.
[19] D.P. Bentz, CEMHYD3D: A Three-Dimensional Cement Hydration and Microstructure Development Modelling Package. Version 2.0 NISTIR 6485, U.S. Department of Commerce, Washington, DC, 1997.
[20] E.J. Garboczi, D.P. Bentz, The effect of statistical fluctuation, finite size error, and digital resolution on the phase percolation and transport properties of the NIST cement hydration model, Cem. Concr Res. 31 (10) (2001) 1501–1514.
[21] P. Navi, C. Pignat, Simulation of cement hydration and the connectivity of the capillary pore space, Adv. Cem. Based Mater. 4 (1996) 58–67.
[22] P. Navi, C. Pignat, Three-dimensional characterization of the pore structure of a simulated cement paste, Cem. Concr. Res. 29 (4) (1999) 507–514.
[23] W.T. Elam, A.R. Kerstein, J.J. Rehr, Critical properties of the void percolation problem for spheres, Phys. Rev. Lett. 52 (1984) 1516–1519.
[24] E.J. Garboczi, J.W. Bullard, Shape analysis of a reference cement, Cem. Concr. Res. (2004)1999 (in press).
[25] E.J. Garboczi, D.P. Bentz, Computer simulation and percolation theory applied to concrete, in: D. Stauffer (Ed.), Annual Reviews of Computational Physics, vol. VII, World Scientific Publishing, Singapore, 1999, pp. 85–123.
[26] R.A. Cook, K.C. Hover, Mercury porosimetry of hardened cement pastes, Cem. Concr. Res. 29 (6) (1999) 933–943.
[27] T.C. Powers, T.L. Brownyard, Studies of the physical properties of hardened portland cement paste, J. ACI (1947) 43.
[28] D.P. Bentz, Three-dimensional computer simulation of Portland cement hydration and microstructure development, J. Am. Ceram. Soc. 80 (1) (1997) 3–21.